Meso-scale Simulations of Compaction Waves in a Granular Bed

R. Menikoff
Theoretical Division, Los Alamos National Laboratory, Los Alamos, NM 87545, USA

Abstract: A granular bed provides an extreme example of a heterogeneous material. Behind a moderate strength wave, the shock compression in a granular material is due to squeezing out pore space rather than an increase in the density of individual grains. This type of shock is known as a *compaction wave*. The key properties of compaction waves are displayed in *meso-mechanics simulations* — continuum mechanics calculations in which individual grains are resolved. Fluctuations in hydrodynamic quantities occur behind the wave front due to stress concentrations at the contact between grains exceeding the yield strength and leading to localized plastic flow. Nevertheless, average wave profiles have the appearance of a dispersed shock wave, and for the most part the fluid mechanics equations, with the addition of a porosity variable, can be used as a homogenized model to describe the behavior of a granular bed. However, some aspects of the wave structure are not accounted for by the homogenized model. These include dispersion of weak waves and an elastic precursor for intermediate strength waves.

Key words: Compaction wave, Wave profile, Meso-scale simulations

1. Introduction

A granular bed is a heterogeneous material. It can support porosity under a compressive load due to the material strength of the grains. However, when the local stress at contacts between grains exceeds the yield strength, the grains deform plastically. The change in shape of the grains allow them to pack together more tightly, thus, decreasing the porosity of the bed. Typically, the yield strength is much less than the bulk modulus. Consequently, for shock pressures up to the yield strength, the compression is almost entirely due to the decrease in porosity rather than an increase in the density of the grains. Such waves are called *compaction waves*.

Frequently, a compaction law relating porosity to pressure is assumed, and the state behind the compaction front is determined by the usual gas dynamic Hugoniot jump conditions. However, the material heterogeneities give rise to fluctuations in the hydrodynamic variables which can affect the wave propagation. Numerical solutions of the continuum mechanics equations which resolve individual grains, known as *meso-scale simulations*, are used to study the structure of compaction waves.

Two-dimensional simulations are initialized with tightly-packed randomly distributed grains, resulting in a granular bed with a porosity of 19%. The constitutive properties of the grains are modeled with a hydrostatic pressure and an elastic-plastic stress deviator for the material strength. A piston boundary condition is used to drive a compaction wave. Despite the fluctuations that arise when an inhomogeneous bed is compressed, a compaction wave profile (averaged in the transverse direction) has the appearance of an ordinary one-dimensional shock profile.

As the wave strength is varied, three types of compaction waves occur: (i) partly compacted dispersive wave, (ii) fully compacted wave with an elastic precursor, (iii) strong shock-like wave. The different wave types show that the response of a heterogeneous material does not simply correspond to a homogeneous material with an average equation of state.

In fact the motivation for these calculations is to understand better the initiation sensitivity of granular explosives. The strong temperature dependence of the reaction rate greatly emphasizes the importance of fluctuations.

2. Homogenized model

For engineering calculations, a practical cell size is typically much larger than the grain size. This is a principal motivation for using a homogenized model to simulate granular flow. A thermodynamically consistent model can be derived as a limiting case of two phase flow (Baer & Nunziato 1986, Menikoff & Kober 2000). The result is a variant of the P–α model (Herrmann 1969, Carroll & Holt 1972).

The model consists of the Euler equations

$$\partial_t \begin{pmatrix} \rho \\ \rho u \\ \rho E \end{pmatrix} + \partial_x \begin{pmatrix} \rho u \\ \rho u^2 + P \\ \rho u E + u P \end{pmatrix} = \vec{\mathbf{0}} \,, \qquad (1)$$

together with an equation for the evolution of the poros-

ity or compaction dynamics

$$(\partial_t + u\partial_x)\phi = \frac{\phi(1-\phi)}{\mu_c}\Big(P_s - \beta\Big) \ . \qquad (2)$$

Here u is the particle velocity, $\rho = 1/V$ is the density, $E = e + \frac{1}{2}u^2$ is the total energy and ϕ is the solid volume fraction (1−porosity). The constitutive relation of the granular bed is characterized by an equation of state

$$P(V, e, \phi) = \phi P_s(\phi V, e) \ , \qquad (3)$$

and an equilibrium compaction law

$$P_s = \beta(\phi) \ , \qquad (4)$$

where P_s is the pressure for the solid grains, and β is the *configuration pressure*. In addition, μ_c is a relaxation parameter with dimensions of viscosity.

The model equations are hyperbolic. The shock locus is determined by the standard Hugoniot equation

$$e - e_0 = \frac{1}{2}(P + P_0)(V_0 - V) \ , \qquad (5)$$

plus the equilibrium condition, Eq. (4). Since the compaction dynamics has the form of a relaxation equation, weak shock waves are dispersed while stronger shock waves are partly dispersed. The homogenized model is adequate for strong wave, but as the meso-scale simulations presented below show, misses qualitative properties of weaker waves.

3. Numerical Model

Meso-scale simulation are performed with an Eulerian continuum mechanics code developed by David Benson at the University of California, San Diego. A similar code has been used previously to study sintering or dynamic compaction of powdered metals (Benson et al. 1997) The initial configuration for the two-dimensional simulations is shown in Fig. 1. The granular bed is chosen to have tightly packed, randomly distributed circular grains. The grains have a mean diameter of 140 μm with a uniform variation of ±10%. The computational domain is 5.15 mm×1.5 mm, and corresponds to a length of about 30 grains and a width of 10 grains. A cell size of 10 μm is used in the simulations. This gives a resolution of 14 cells per grain.

Periodic boundary conditions are used for the top and bottom. Compaction waves are driven by a piston at the right boundary. We note that the porosity profile, smoothed by taking a running average over two grain diameters, shows a small amplitude variation with a mm scale wavelength. The resulting density variations of the bed leads to variations in hydrodynamical

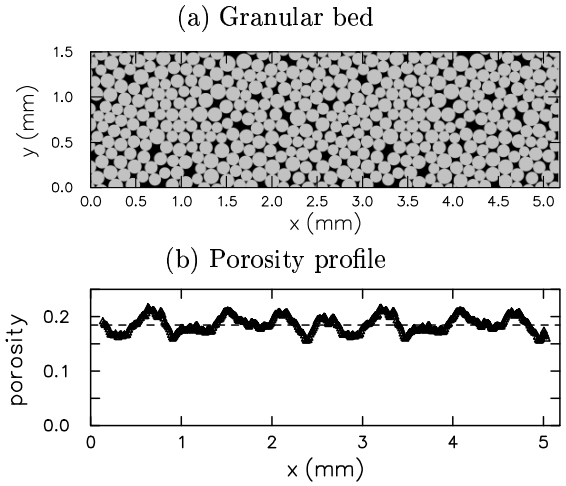

Figure 1. Initial configuration. (a) Grey represents grains and black represents pores. (b) The porosity profile is averaged over a length of two grain diameters. Average porosity of 19 % is shown as dashed line.

quantities behind the front of a propagating compaction wave.

A hydrostatic equation of state (EOS) plus an elastic-plastic strength model are used for the constitutive relation of the grains. The EOS is of the Mie-Grüneisen form with a reference curve based on a linear u_s–u_p fit to the principal shock Hugoniot. The strength model is isentropic with a constant shear modulus and von Mises yield strength for rate independent plasticity.

The properties of the grains are chosen to correspond to HMX (cyclo-tetramethylene-tetranitramine). Though HMX is an explosive, here we focus on mechanical properties and treat the grains as non-reactive. The constitutive parameters are listed in Table 1. The packing algorithm, constitutive relations and previous compaction wave simulations are described in Menikoff & Kober 1999.

4. Simulations of Compaction Waves

The pressure scale for compaction is set by the yield strength of the grains. Depending on the wave pressure relative to the yield strength, three types of compaction waves occur. An example of each wave type

Table 1. *Constitutive parameters of grains.*

c_0	2.65	km/s	Bulk sound speed
s	2.38	—	Slope of u_s–u_p relation
Γ/V	2.09	g/cm^3	Grüneisen coefficient
ρ_0	1.9	g/cm^3	Initial density
G	10.0	GPa	Shear modulus
Y	0.37	GPa	Yield strength

(a) Stress field.

(b) Stress profile.

(c) Porosity profile.

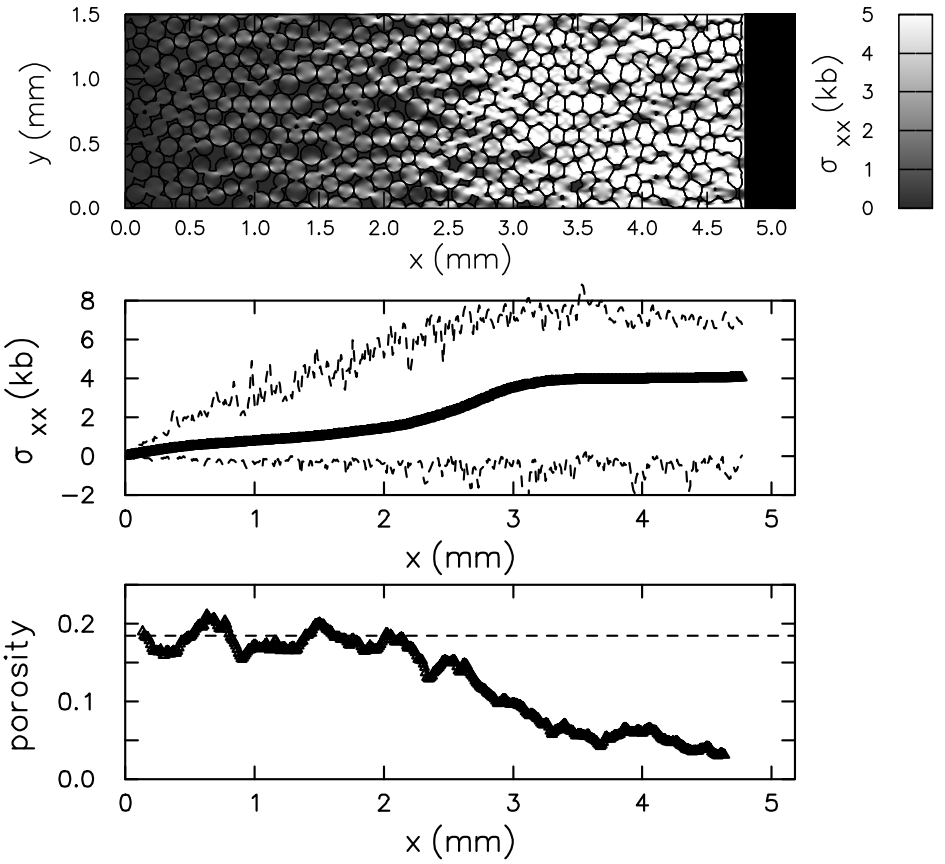

Figure 2. Weak, dispersive compaction wave. Piston velocity of 200 m/s and time of 2.0 μs. (a) The black region on the right indicated the distance the piston has traveled, and the solid lines represent interfaces of the grains. (b) Dashed lines correspond to minimum and maximum values. (c) Dashed line represents the initial porosity.

is illustrated with the meso-scale simulations presented below. Other calculations, not presented here, show that the results are not affected by doubling the spatial resolution of the mesh.

4.1. Weak, dispersive compaction wave

The case of a weak wave is shown in Fig. 2. Several features of the flow are noteworthy. (i) A fingering pattern is evident in the two-dimensional plot of the stress field. This is the analog of *stress bridging* that is observed for a granular bed under static compression. (ii) Despite the fluctuations in the stress field, the average profile is smooth. Thus, on a coarse grain scale the wave is one-dimensional in character. (iii) The wave is only partly compacted. The compaction is due to the distortion in the grains when stress concentrations exceed the yield strength. (iv) The wave is not steady but spreads out as it propagates. This occurs because, as shown in Fig. 3, the energy behind the wave front exceed the Hugoniot energy, Eq. (5), for a steady wave.

The dissipative energy in this case is dominated by plastic work. The plastic dissipation depends on the

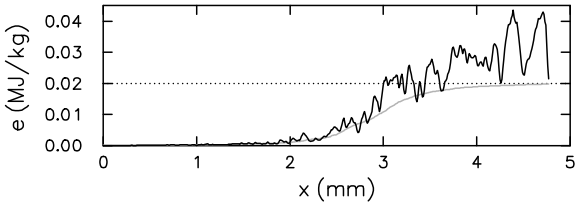

Figure 3. Energy profiles for weak compaction wave shown in Fig. 2. Solid black line is specific internal energy. Grey line is specific kinetic energy. Dotted line is kinetic energy based on piston velocity, which is nearly the same as the corresponding internal energy on the Hugoniot.

stress concentrations which determines the distortion of the grains. Consequently, the dissipation depends on the change in porosity. In contrast to viscous dissipation for a gasdynamic shock, the plastic dissipation can not be scaled by varying the width of the wave profile.

4.2. Compaction wave with precursor

As the piston velocity increases, the stress behind the wave increases resulting in more plastic flow and a de-

(a) Stress field.

(b) Stress profile.

(c) Porosity profile.

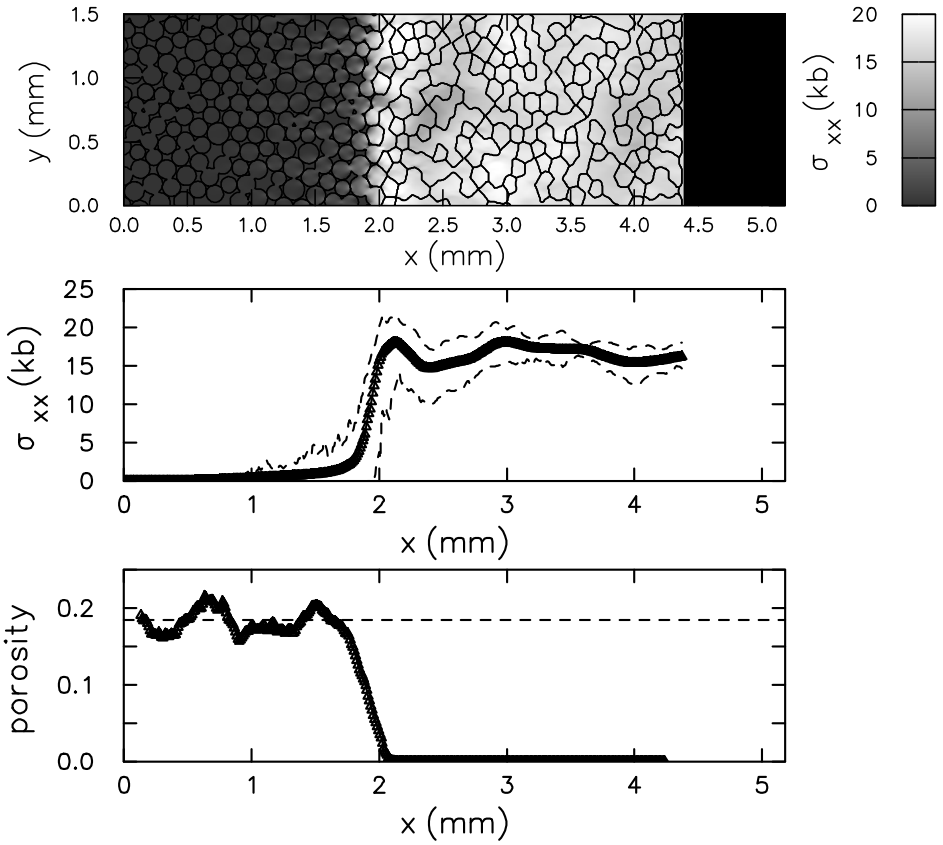

Figure 4. Intermediate, compaction wave with precursor. Piston velocity of 500 m/s and time of 1.6 μs. (a) The black region on the right indicated the distance the piston has traveled, and the solid lines represent interfaces of the grains. (b) Dashed lines correspond to minimum and maximum values. (c) Dashed line represents the initial porosity.

(a) Stress profile.

(b) Equivalent plastic stress.

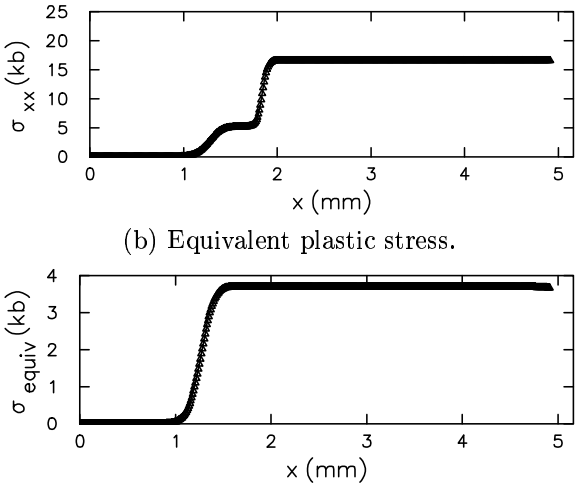

Figure 5. Split wave in homogeneous elastic-plastic medium; elastic precursor followed by plastic shock. Piston velocity of 250 m/s at time of 1 μs.

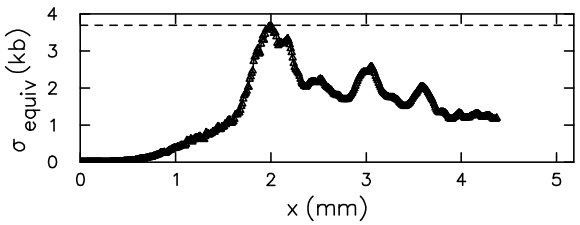

Figure 6. Equivalent plastic stress for compaction wave for compaction wave shown in Fig. 4. Dashed line represents the yield strength.

crease in porosity. When the stress is large compared to the yield strength, the porosity limits to zero and the wave is *fully compacted.* This case is shown in Fig. 4. The characteristic feature in this regime is a weak precursor ahead of the main wave.

The wave structure results from the elastic-plastic transition in the grains. It is analogous to a split wave in a homogeneous material. With the same constitutive properties and at a similar pressure, the stress profiles are shown in Fig. 5. The lead wave is the elastic precursor, and is followed by a plastic wave. Experimentally the rise time of the precursor is much shorter than that of the plastic wave. In the numerical solution, the width

(a) Stress field.

(b) Stress profile.

(c) Porosity profile.

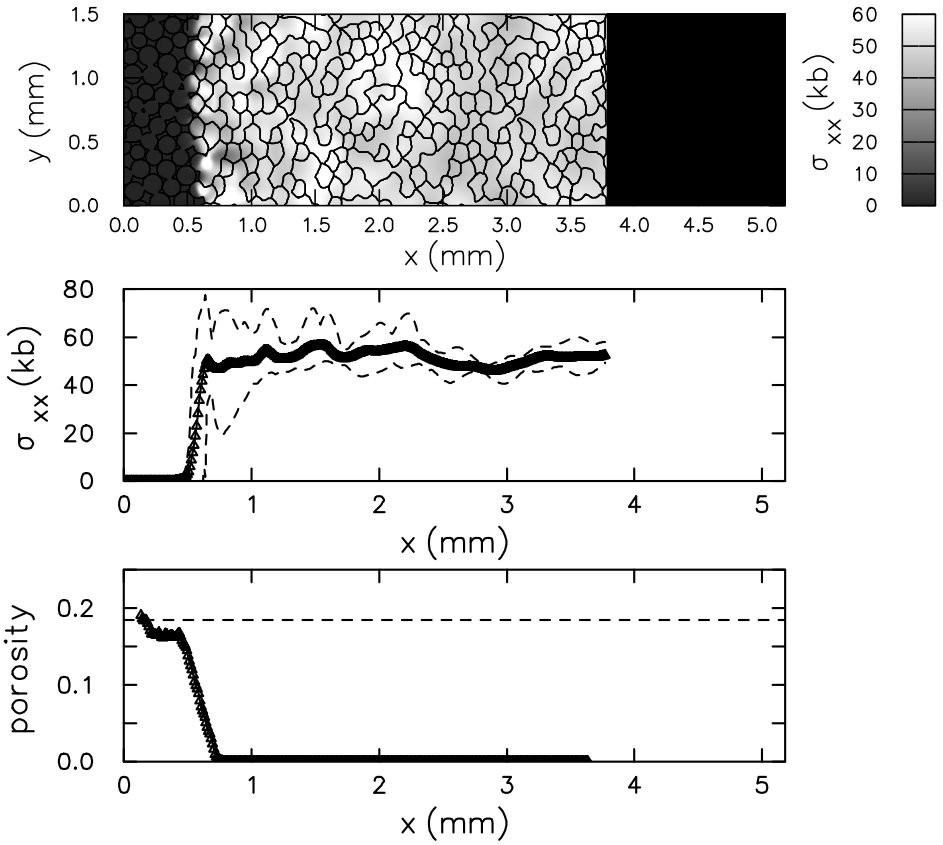

Figure 7. Strong, shock-like compaction wave. Piston velocity of 1000 m/s and time of 1.4 μs. (a) The black region on the right indicated the distance the piston has traveled, and the solid lines represent interfaces of the grains. (b) Dashed lines correspond to minimum and maximum values. (c) Dashed line represents the initial porosity.

of the elastic wave is artificially large since the Mach number is close to 1, resulting in a weak convergence of the characteristics. The width of the plastic wave is artificially short as a consequence of the simplified rate independent model for the plastic flow.

Several features of the wave structure result from heterogeneities in the granular bed. (i) The speed of the toe of the precursor is lower than the longitudinal sound speed of the grains. This is a consequence of the elastic stress being transmitted only through the contact between grains. The additional path length for a signal decreases the effective elastic wave speed. (ii) The precursor is spread out rather than shock-like. This is a consequence of the stress concentrations which results in localized plastic flow in contrast to the sudden onset of plastic flow in the homogeneous case. The spread of the plastic flow is seen in the plots of the equivalent plastic stress, Figs. 5b and 6. (iii) Moreover, Fig. 6 shows that the equivalent plastic stress decays behind the plastic wave front where the porosity decreases to zero. This is probably due to the fact that the grains can adjust their position to relieve shear stress. The equilibration rate is slow since the particle velocity is much less the wave speed. Very likely the decay could be account for with a visco-elastic model. The shear stress is not included in the homogenized model of section 2., and leads to a small error in computing the state behind a compaction wave based on the Hugoniot Eq. (5) and the equilibrium condition Eq. (4).

4.3. Strong, shock-like compaction wave

As the piston velocity is increased further, the speed of the plastic wave front increases and eventually exceeds the elastic sound speed. When this occurs, just as in the case of a homogeneous elastic-plastic material, the plastic wave outruns the elastic precursor resulting in a single shock-like wave profile, as shown in Fig. 7.

Two features of the compaction wave are noteworthy: (i) Despite the inhomogeneities resulting from the porosity of the bed, the wave front is nearly planar, to within a grain diameter; (ii) The width of the wave profile is on the order of a grain diameter. To show the numerical resolution of the calculation, a simulation was performed of a shock in a homogeneous material with the same elastic-plastic constitutive relation

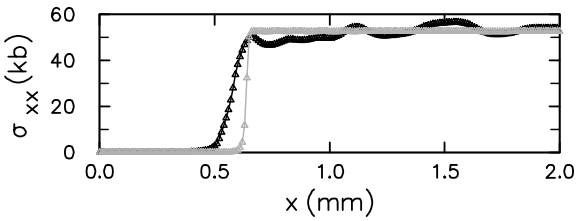

Figure 8. Comparison of wave profiles. Black is shock in granular bed and gray is shock in homogeneous medium. Both shocks are driven by a 1000 m/s piston. To facilitate the comparison of the width of the profiles, the shock profile for the homogeneous case has been scaled to match the amplitude of the granular profile, and the times are chosen such that both waves have propagated the same distance.

on a mesh with the same cell size. The wave profiles are compared in Fig. 8. This demonstrates that the heterogeneous length scale, namely the grain diameter, is determining the wave width and not the numerical resolution of the computation.

5. Summary

The meso-scale simulations show that compaction waves in a granular bed have a one-dimensional character. The transverse averaged wave profiles are smooth. Moreover, the wave speed and the state behind the wave front are consistent with the standard Hugoniot jump relations. There is a small discrepancy due to the difference between the normal component of stress σ_{xx} and the pressure P. Thus, compaction waves can be described by a homogenized model. However, the constitutive relations would have to be modified to account for the dispersive nature of weak waves and the smearing out of the elastic precursor for intermediate strength waves.

Some simplifying aspects of the meso-scale model affect the structure of compaction waves being simulated. Foremost is the fact that the calculations are two-dimensional while in reality a granular bed is three-dimensional. The dimensionality affects the packing of the grains, in particular, the minimum porosity and the distribution of contacts between grains. The latter determines the stress concentrations and would affect the change in porosity for a given wave strength.

The simulations show that the minimum width of a wave is determined by the size of the grains. However, experiments show that for sufficiently small grains, compaction waves have a minimum rise time (Sheffield, Gustavsen & Anderson 1997, Fig. 2.10). This breaks the scaling with grain size. The time scale come from the fact that plasticity is really rate dependent rather than the rate independent model used in the simulations.

The detailed structure of the profile, in particular the fluctuations, depends on the dissipation mechanism. The simulation reported here have three dissipative mechanisms: plastic work, shear viscosity and an artificial bulk viscosity. Conspicuously absent is friction between grains. The difficulty is that Eulerian algorithms can handle the large distortion of grains but lose accuracy at interfaces.

Two other properties are not included in the simplified model. Grains are little crystal and have anisotropic elastic properties. Also, grains are subject to fracture for weak wave that are not fully compacted. All these effects are important for application such as determining the initiation sensitivity of a damaged explosive.

Acknowledgement. Funding for this research from the U.S. Dept. of Energy under contract W-7405-ENG-36. The author thanks Prof. David Benson, Univ. of Calif., San Diego, for making his code available. This article is based on previous work done in collaboration with Ed Kober.

References

Baer M.R., Nunziato J.W. (1986) A Two-Phase Mixture Theory for the Deflagration-to-Detonation Transition in Reactive Granular Materials, Int. J. Multiphase Flow 12:861–889.

Benson D.J., Nesterenko V. F., Jonsdottir F., Meyers M. A. (1997) Quasi-static and Dynamic Regimes of Granular Material Deformation under Impulse Loading. J. Mech. Phys. Solids 45:1955–1999.

Carroll M., Holt A.C. (1972) Suggested Modification of the P–α Model for Porous Materials, J. Applied Phys., 43:759–761.

Herrmann W. (1969) Constitutive Equation for the Dynamic Compaction of Ductile Porous Material, J. Applied Phys., 40:2490–2499.

Menikoff R., Kober, E. (1999) Compaction Waves in Granular HMX, Los Alamos National Laboratory technical report LA-13546-MS, parts I and II: http://lib-www.lanl.gov/la-pubs/00326750.pdf, http://lib-www.lanl.gov/la-pubs/00326751.pdf.

Menikoff R., Kober, E. (2000) Equation of State and Hugoniot Locus for Porous Materials: P–α Model Revisited, in **Shock Compression of Condensed Matter – 1999**, eds. Furnish M.D., Chhabildas L.C., Hixson R.S. (APS, NY) 129–132.

Sheffield S.A., Gustavsen R.L., Anderson M.U. (1994) Shock Loading of Porous High Explosives, in **High-Pressure Shock Compression of Solids IV: Response of Highly Porous Solids to Shock Compression**, eds. Davison L., Horie Y., Shahinpoor M. (Springer-Verlag, NY) 23–61.